



Characterization of Surface Spectral Emissivity Retrieved from EE9-FORUM Simulated Measurements

Cristina Sgattoni¹ · Marco Ridolfi² · Chiara Zugarini¹ · Luca Sgheri¹

Received: 6 October 2023 / Revised: 26 January 2024 / Accepted: 29 January 2024 / Published online: 23 February 2024
© The Author(s) 2024

Abstract

FORUM (Far-infrared Outgoing Radiation Understanding and Monitoring) has been approved to be the ninth Earth Explorer mission of the European Space Agency and is scheduled for launch in 2027. The core FORUM instrument is a Fourier transform spectrometer, which will, for the first time, measure the upwelling spectral radiance in the far-infrared (FIR) and mid-infrared (MIR) portions of the Earth's spectrum. These radiances will be processed up to level 2, to determine mainly the vertical profile of water vapor, surface spectral emissivity, and cloud parameters. In this paper, we assess the performance of the FORUM surface spectral emissivity product based on all-sky sensitivity study. In the FIR, we find that the retrieval error is mainly driven by the precipitable water vapor (PWV) in clear-sky conditions. In dry atmospheres, FIR emissivity can be retrieved with an error less than 0.01. In cloudy conditions, small errors can be achieved for optically thin clouds, especially for small values of the PWV. In the MIR, we observe that a large thermal contrast between the surface and the lowest atmospheric layers increases the sensitivity of the measurements to the surface emissivity in clear-sky conditions and an emissivity retrieval error less than 0.01 can usually be achieved. In cloudy conditions, small errors can be achieved for optically thin clouds, especially for large values of the surface temperature. Applying a coarser retrieval grid further reduces retrieval error, at the expense of an increased emissivity smoothing error.

Keywords Remote sensing · Retrieval of geophysical parameters · Far infrared · Surface spectral emissivity · FORUM

1 Introduction

At least 50% of the Earth's total clear-sky long-wave cooling to space takes place within the far-infrared (FIR) spectral range [1, 2]. In the presence of clouds, this fraction is even larger [3], as clouds imply lower emitting temperatures,

causing a shift towards longer wavelengths in the peak of black-body emission. The FIR region is particularly sensitive to variations of water vapor abundance in the upper troposphere/lower stratosphere (UTLS) region because it includes the spectral signatures of the rotational band of the water vapor [1]. Moreover, the FIR region is also sensitive to the presence of ice clouds. Cirrus clouds (optically thin ice clouds) influence the Earth's energy budget by reflecting back to space the incoming solar radiation (cooling effect) and trapping the long-wave emissions into the atmosphere (warming effect). The relative impact of these effects depends on cloud optical and micro-physical properties [4, 5]. The FIR portion of the spectrum is also sensitive to ice particle size and habit [6–8].

For these reasons, monitoring the behavior of the spectrally resolved FIR radiances is an important tool to validate climate models and to study climate changes [9–11]. Despite the significance, no direct observations are available so far. FORUM (Far-infrared Outgoing Radiation Understanding and Monitoring) is a Fourier transform spectrometer (FTS) that will measure at nadir from space the upwelling spectral

✉ Cristina Sgattoni
cristina.sgattoni@fi.iac.cnr.it

Marco Ridolfi
marco.ridolfi@cnr.it

Chiara Zugarini
chiara.zugarini@fi.iac.cnr.it

Luca Sgheri
luca.sgheri@cnr.it

¹ Istituto per le Applicazioni del Calcolo (IAC), Consiglio Nazionale delle Ricerche (CNR), Via Madonna del Piano, 10, Sesto Fiorentino I-50019, FI, Italy

² Istituto Nazionale di Ottica (INO), Consiglio Nazionale delle Ricerche (CNR), Via Madonna del Piano, 10, Sesto Fiorentino I-50019, FI, Italy

radiance emitted by the Earth from 100 to 1600 cm^{-1} , with a planned resolution of 0.5 cm^{-1} . FORUM has been selected by the European Space Agency [12] to be the ninth Earth Explorer mission, with a launch date expected in 2027.

FORUM's main targets include water vapor profiles, surface spectral emissivity in polar regions, ice cloud properties, and spectral fluxes. The retrieval of surface spectral emissivity has also been examined earlier in the literature. In [13–15], the final retrieval error is examined in clear-sky conditions, considering a database of cases organized into latitude bands. In this study, we investigate in more detail the sensitivity of measurements to surface spectral emissivity across various scenarios spanning all latitudes under clear-sky conditions. Additionally, we assess this sensitivity also in the presence of clouds in Antarctica. The distinctive aspects of this work lie in the diversity of considered scenarios, encompassing different surface types, precipitable water vapor levels, and surface temperatures. Furthermore, our analysis extends to cloudy scenarios, marking a significant advancement in the understanding of spectral emissivity retrieval under various atmospheric conditions. The study is based on synthetic FORUM measurements obtained from realistic observational scenarios.

The paper is organized as follows. Section 2 defines the method used to characterize the performance of the emissivity product. In Section 3, we introduce the main characteristics assumed for the FORUM measurements. Section 4 presents the atmospheric and surface scenarios for which we performed the sensitivity study. Sections 5 and 6 illustrate the results of the analysis for the clear and cloudy scenarios, respectively. In Section 7, we perform test retrievals illustrating the trade-off between random and smoothing errors obtained by changing the emissivity retrieval grid step size. Finally, in Section 8, we present a summary of the work and draw the conclusions.

2 Method

We simulate the performance of the optimal estimation [16] solution that corresponds to the minimum of the cost function ξ^2 :

$$\xi^2(\mathbf{x}) = (\mathbf{y} - \mathbf{f}(\mathbf{x}))^T \mathbf{S}_y^{-1} (\mathbf{y} - \mathbf{f}(\mathbf{x})) + (\mathbf{x} - \mathbf{x}_a)^T \mathbf{S}_a^{-1} (\mathbf{x} - \mathbf{x}_a), \quad (1)$$

where \mathbf{y} is the measurement vector with associated error covariance matrix \mathbf{S}_y , $\mathbf{f}(\mathbf{x})$ is a radiative transfer model simulating the measurement \mathbf{y} from the atmospheric, cloud and surface state \mathbf{x} . The vector \mathbf{x}_a is an a priori estimate of \mathbf{x} , with

error covariance matrix \mathbf{S}_a . Let $\hat{\mathbf{x}}$ be the minimum of Eq. 1, and \mathbf{K} the Jacobian matrix of the model $\mathbf{f}(\mathbf{x})$. The covariance matrix \mathbf{S}_x of the solution $\hat{\mathbf{x}}$ can be calculated from \mathbf{S}_y using the linear propagation of errors as

$$\mathbf{S}_x = \left(\mathbf{K}^T \mathbf{S}_y^{-1} \mathbf{K} + \mathbf{S}_a^{-1} \right)^{-1}. \quad (2)$$

In our tests, surface spectral emissivity is assumed to be the only component of the unknown state \mathbf{x} . Since the dependence of the radiative transfer model on the emissivity is linear, \mathbf{K} does not depend on \mathbf{x} . Hence, Eq. 2 can be calculated from any emissivity profile \mathbf{x} .

Emissivity is assumed as retrieved at discrete wavenumbers $\omega[j]$, with $j \in (1, \dots, N)$. Given any spectral interval $[\omega_i, \omega_f]$, let $N_{\omega_i}^{\omega_f}$ be the number of grid points such that $\omega[j] \in [\omega_i, \omega_f]$. We calculate the average retrieval error in that interval as

$$\sigma_{\omega_i}^{\omega_f} = \frac{1}{N_{\omega_i}^{\omega_f}} \sum_{j:\omega[j] \in [\omega_i, \omega_f]} \sqrt{(\mathbf{S}_x)_{jj}}. \quad (3)$$

Loosely speaking, if $\left(\mathbf{K}^T \mathbf{S}_y^{-1} \mathbf{K} \right)_{jj} \rightarrow 0$, the measurements are not sensitive to the parameter j . Then, from Eq. 2, $(\mathbf{S}_x)_{jj} \rightarrow (\mathbf{S}_a)_{jj}$, i.e., the error estimate tends to the a priori error. On the other hand, the larger the $\left(\mathbf{K}^T \mathbf{S}_y^{-1} \mathbf{K} \right)_{jj}$, the smaller the $(\mathbf{S}_x)_{jj}$. Thus, $\sigma_{\omega_i}^{\omega_f}$ quantifies the sensitivity of the measurement to the emissivity in the given interval. The sensitivity study of this paper relies on the evaluated retrieval errors, which can be estimated without carrying out a full retrieval.

For the evaluation of the Jacobian \mathbf{K} for each atmospheric, cloud, and surface scenario, we rely on the CLAIM (CLouds and Atmosphere Inversion Module) code. It is an advanced version of the retrieval module used in the FORUM E2E project [13]. The inversion code is based on the LBLRTM (Line By Line Radiative Transfer Model) forward model [17] in clear sky and on an accelerated version [18] of the classical DISORT (DIScrete Ordinate Radiative Transfer) method [19] in cloudy sky. The radiative transfer uses a full-physics approach, with significant computational demands. In this work, however, we prioritize the accuracy of the models over execution time.

3 FORUM Measurement Characteristics

FORUM will fly on a sun-synchronous polar-orbiting satellite. The orbit inclination is planned to be of 98.7°, and the

altitude of about 830 km. The orbit repeat cycle will be 29 days.

The key instrument of the FORUM mission is a FT spectrometer measuring the spectrum of the upwelling Earth's outgoing longwave radiation (OLR) by looking at nadir [12, 20]. To date, the real instrument has not been built yet. Thus, we use the consolidated mission requirements to simulate the measurements. The ground pixel is a circle, with a diameter of approximately 15 km. During the acquisition time (≈ 8 s), the ground pixel is kept fixed by continuously adjusting the pointing angle to compensate for the satellite motion. No across-track scanning is foreseen. The resulting distance between neighboring ground pixels is approximately 100 km. FORUM measured interferograms will be processed to get geolocated and calibrated spectral radiances in the interval from 100 to 1600 cm^{-1} , with a (unapodized) spectral resolution of 0.5 cm^{-1} (full width at half maximum, FWHM of the response function). The sampling step of the spectrum is $\approx 0.36 \text{ cm}^{-1}$. The required NESR (noise equivalent spectral radiance) of the unapodized spectrum is 40 $\text{nW}/(\text{cm}^2 \text{ sr cm}^{-1})$ in the range between 200 and 800 cm^{-1} and 100 $\text{nW}/(\text{cm}^2 \text{ sr cm}^{-1})$ elsewhere. We use these specifications to build S_y . The ARA (absolute radiometric accuracy) of the measured spectral radiance is required to be much smaller than the NESR [12, 14], thus it will be relevant only for the assessment of the error budget of averaged spectra and/or retrieved parameters. Nevertheless, the ARA is considered in our simulations.

4 Measurement Scenarios

The atmospheric, cloud, and surface states that we use as a basis for the evaluation of the performance of the retrieved surface spectral emissivity are extracted from the ECMWF (European Center for Medium-Range Weather Forecast) database ERA5 [21].

In the ERA5 database, surface temperature and vertical profiles of pressure, temperature, water vapor, ozone, cloud ice, and liquid water contents, are supplied on a grid of 60 geopotential levels. At each geolocation, this vertical grid was cut at the estimated pressure of the surface level. Other relevant gases, such as CO_2 , CH_4 , CO , SO_2 , HNO_3 , and NO_2 were also extracted from the ECMWF database. The profiles of the remaining gases needed for an accurate simulation of the upwelling spectral radiances were taken from the IG2 (Initial Guess v2) climatological database [22].

For the cloudy scenarios, the effective radii of ice crystals and water droplets needed to calculate the multiple scattering effect, were modeled according to the Wyser model [23] for ice particles, and according to the Martin model [24] for water droplets.

The dependence of the spectrum on the emissivity is linear, thus the Jacobian does not depend on the emissivity profile itself. However, the Jacobian is computed by the LBLRTM code, that needs anyway the emissivity profile for the calculation of the radiative transfer. To create this input, we used the Huang database [10].

5 Clear Sky Results

The database considered in this study consists of a collection of data covering the entire globe with a longitude and latitude grid step size of 10° and 5° , respectively, corresponding to 1262 grid points. To manage the dataset size, the data only include the first 20 days of July and January in 2021 at 12:00 UTC, resulting in a total of 25240 different atmospheric states for each month. To begin our analysis, we focused on clear-sky conditions. Therefore, for each geolocation, we selected the first clear-sky day available in the database. To determine the scene condition, we computed the total cloud optical depth τ at 900 cm^{-1} from the liquid and ice cloud contents following the method described in Yang et al. [25]. Then, we selected the first day for which τ was found to be less than 0.03. This threshold corresponds to the minimum value for which a cloud can be detected from FORUM spectra, and the perturbation introduced on the spectrum is of the same order of the FORUM random noise [13]. With this condition not all geolocations include a clear-sky case in our database. Figure 1 illustrates our clear-sky dataset, consisting of 528 cases in July and 653 cases in January. For the sake of clarity, in all the maps the graphical symbols for the cases located exactly at the poles are replicated at all longitudes.

For the purpose of our study, we focused on two different intervals of the spectrum. The first region is in the FIR, specifically the range from 300 to 600 cm^{-1} (corresponding to wavelengths from 33.3 to 16.7 microns). In this region, the main absorption is due to the water vapor rotational band [26]. The second region is the main atmospheric window, which spans from 800 to 950 cm^{-1} , (corresponding to wavelengths from 12.5 to 10.5 microns). This region is known for its high transparency in clear-sky conditions.

In our simulations, we used a constant emissivity a priori error of 0.15. We employed a fine and regular retrieval grid for surface emissivity, with a step size of 5 cm^{-1} , resulting in 301 grid points across the entire FORUM spectrum and 61 and 31 points within our specific windows.

Figures 2 and 3 show the values of σ_{300}^{600} and σ_{800}^{950} for our sample sets in July and January, respectively.

From panels (b) of the figures we note that in the atmospheric window, the error is low at all latitudes, as expected for clear-sky conditions.

On the other hand, in the FIR region, the measurements exhibit the largest sensitivity to emissivity at polar latitudes,

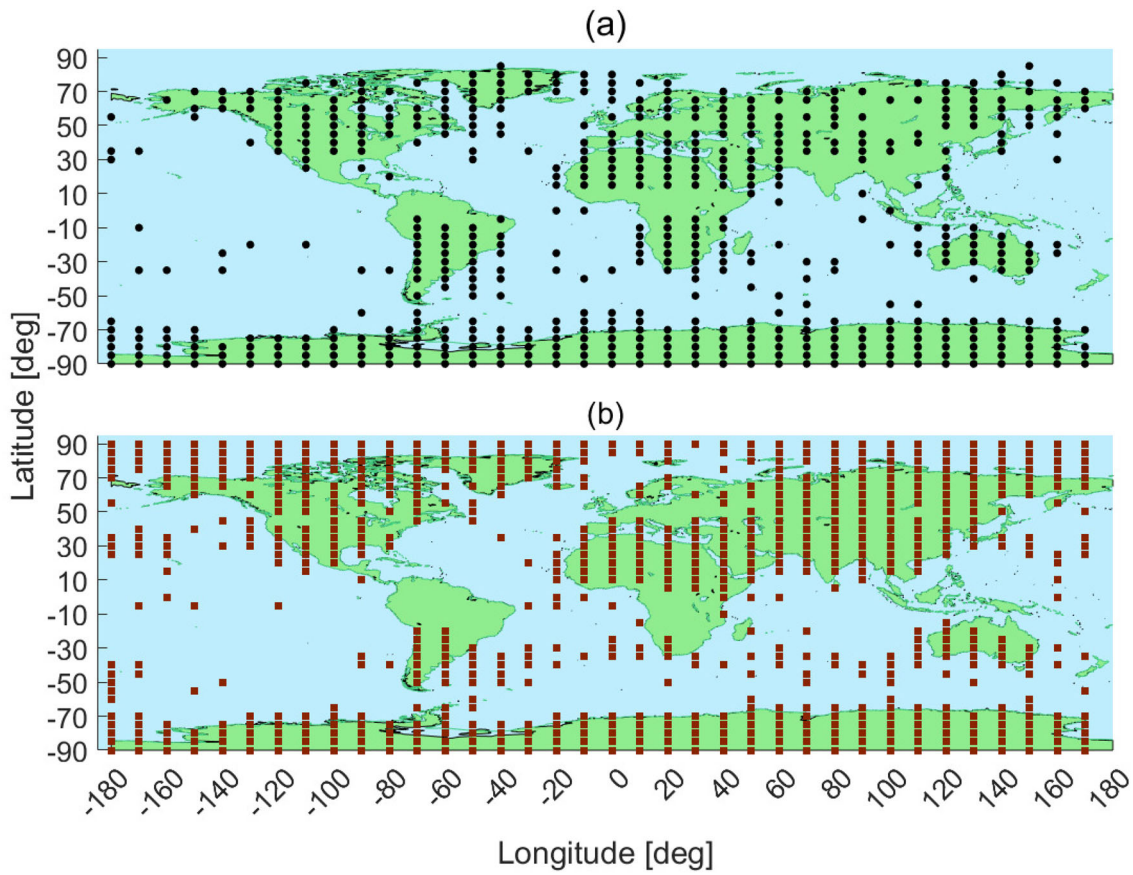


Fig. 1 Tested clear-sky cases in July (a) and January (b), represented by the black circles and red squares, respectively

Fig. 2 Surface emissivity average error in the specific spectral bands 300–600 cm⁻¹ (a) and 800–950 cm⁻¹ (b) in July 2021 at 12:00 UTC

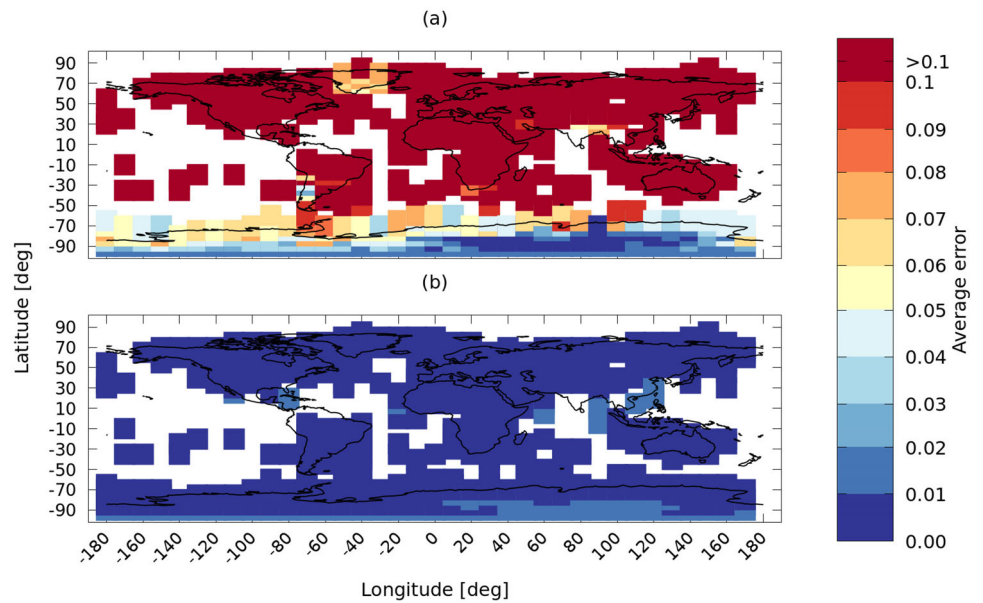
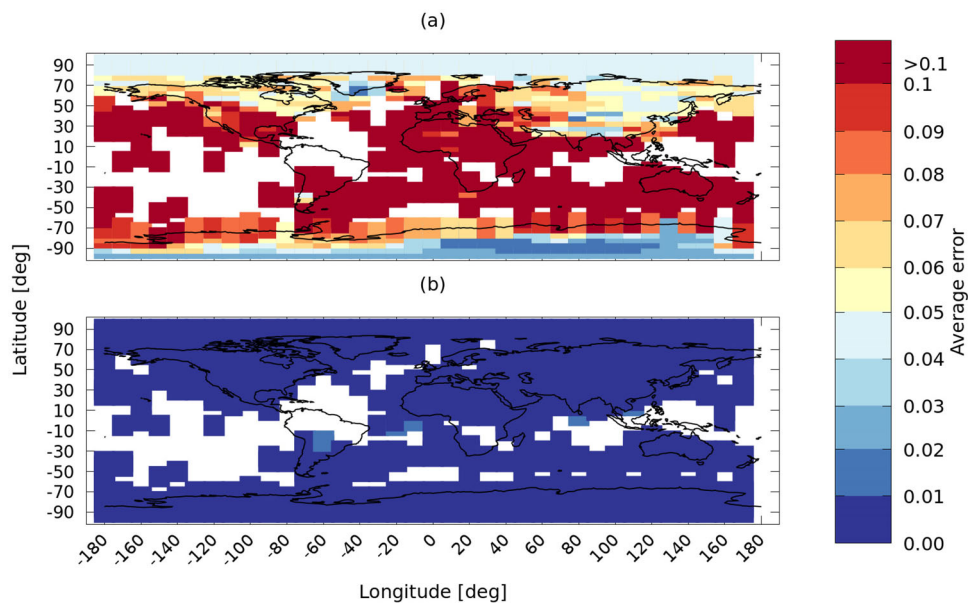


Fig. 3 Surface emissivity average error in the specific spectral bands 300–600 cm⁻¹ (a) and 800–950 cm⁻¹ (b) in January 2021 at 12:00 UTC



where the retrieval error is less than 0.08. At other latitudes, the sensitivity is low, with the error approaching its a priori bound at the tropics.

The primary factor contributing to the different sensitivity is the amount of precipitable water vapor (PWV), which is low in the polar regions and higher elsewhere, as shown in Fig. 4. Note that a marked seasonality of PWV is observed in the northern polar region. On the Antarctic plateau, on the other hand, the PWV remains below 1 mm all year round.

The PWV is not the only factor that influences the emissivity retrieval error. Figure 5 shows that the main driver of the FIR emissivity error is indeed the PWV, with the surface temperature playing a secondary role.

In the atmospheric window, the main driver of the emissivity retrieval error is the surface temperature, while the PWV plays a secondary role, as shown in Fig. 6.

6 Cloudy Sky Results

The cloudy sky analysis presented in this section is based on a database with a smaller size compared to that used in Section 5. This reduction in size was necessary due to the significant computational time required for each individual sensitivity calculation since in cloudy conditions multiple scattering must be simulated. For this analysis, we focused

Fig. 4 PWV for our sample sets in July 2021 (a) and January 2021 (b) at 12:00 UTC

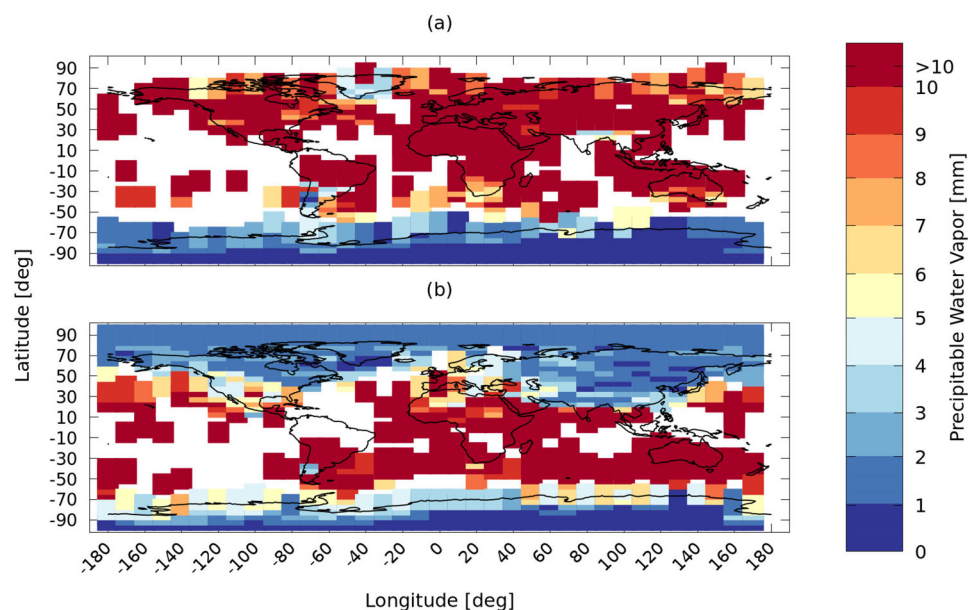
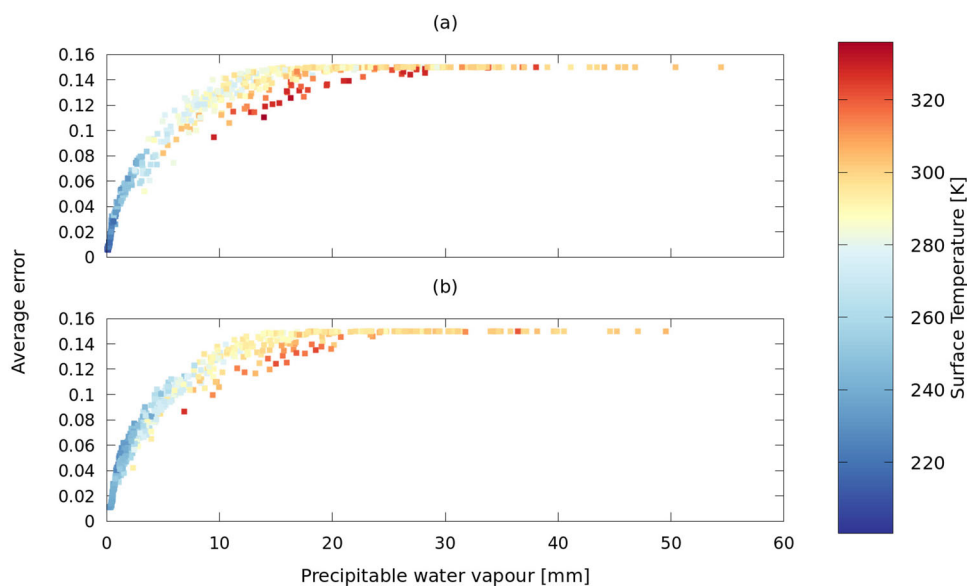


Fig. 5 Surface emissivity average error in the FIR spectral region versus PWV. The corresponding surface temperature is color coded. July 2021 dataset is shown in (a), January 2021 dataset in (b)



on the Antarctic region, which, as indicated by the results of Section 5, exhibits a larger sensitivity to surface emissivity. The ERA5 latitude-longitude grid contains 145 grid points with latitude of -70° or less. In order to capture the seasonal variation, we considered the first 20 days of both January and July 2021 at 12 : 00 UTC. Thus, the sample is composed of 2900 different atmospheric states for each month.

We first exclude clear-sky cases, identified by $\tau < 0.03$, as explained in Section 4. Cases with $\tau > 10$ are also excluded as the measurements are not sensitive to surface properties. Then, we select a subset of the remaining cases, focused mainly on small values of τ . The cloud properties for the cases in the sample with $\tau \leq 1$ are listed in Table 1 for July and in Table 2 for January. Note that during the July winter

season, there are only ice clouds, whereas in the January summer season, there are also some liquid clouds.

The geographical distribution of the specific selected cases is shown in Fig. 7. Cases located exactly at the pole are replicated at each longitude for the sake of visual clarity.

We used the same settings for the simulations as in Section 5, with a constant a priori error of 0.15 and the fine retrieval grid for emissivity with a 5 cm^{-1} step. Figures 8 and 9 show the results for the FIR and the atmospheric window regions, respectively.

We note that, as expected, in both regions the main factor determining the retrieval error is the cloud optical depth. However, the main factors determining the retrieval errors in clear-sky cases, still play an important role in cloudy con-

Fig. 6 Surface emissivity average error in the atmospheric window versus surface temperature. The corresponding PWV is color coded. July 2021 dataset is shown in (a), January 2021 dataset in (b)

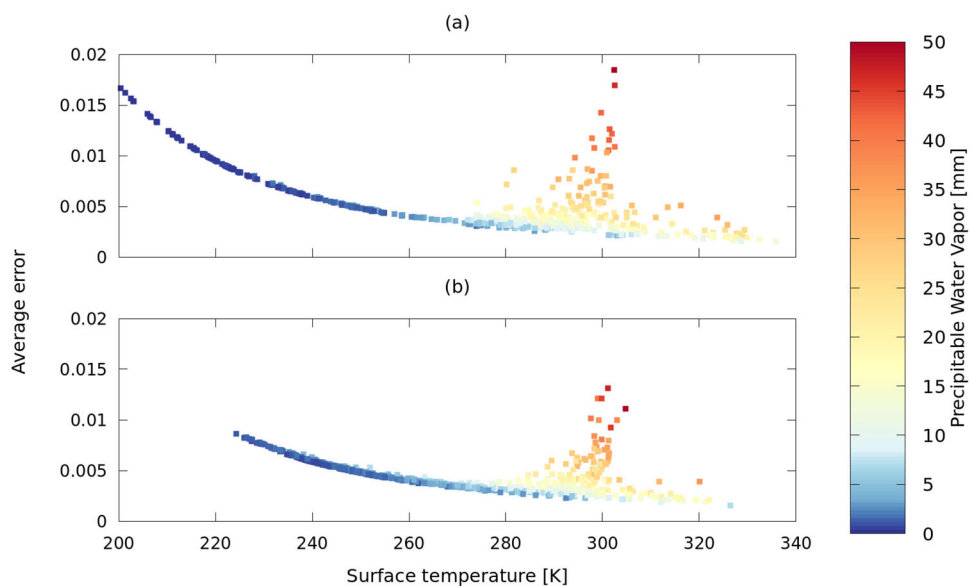


Table 1 Cloud properties for the July dataset, reporting geolocation (LON/LAT), day number (DAY), total optical depth due to clouds (τ), and number of clouds (NC)

LON	LAT	DAY	τ	NC	CL1	CL2	CL3
80	−80	1	0.030	1	I: [3.994,4.814], 2	N/A	N/A
−160	−85	19	0.044	1	I: [1.130, 3.076], 6	N/A	N/A
−60	−75	7	0.062	2	I: [0.007,0.246], 2	I: [9.579,11.666], 3	N/A
−100	−80	18	0.080	1	I: [2.082,2.590], 2	N/A	N/A
50	−85	1	0.102	2	I: [3.337, 3.598], 1	I: [4.184, 6.276], 3	N/A
N/A	−90	20	0.130	1	I: [2.783,4.260], 3	N/A	N/A
110	−80	16	0.142	3	I: [3.330,3.859], 1	I: [4.467,7.478], 4	I: [8.435,10.131], 2
N/A	−90	2	0.167	1	I: [2.784,4.248], 3	N/A	N/A
−30	−75	14	0.182	1	I: [0.133,1.532], 7	N/A	N/A
20	−80	4	0.218	1	I: [3.147, 6.453], 5	N/A	N/A
−100	−75	2	0.272	1	I: [1.718,7.285], 9	N/A	N/A
170	−80	18	0.288	1	I: [0.051,3.596], 13	N/A	N/A
−110	−80	5	0.369	1	I: [1.812,4.871], 6	N/A	N/A
N/A	−90	4	0.424	1	I: [2.785,5.668], 5	N/A	N/A
100	−80	1	0.477	1	I: [3.619,6.258], 4	N/A	N/A
70	−80	15	0.577	1	I: [4.363,9.379], 6	N/A	N/A
−80	−85	4	0.605	1	I: [1.263,3.620], 7	N/A	N/A
−80	−80	10	0.692	1	I: [2.183,7.466], 8	N/A	N/A
120	−85	6	0.797	1	I: [2.987,5.694], 5	N/A	N/A
160	−80	20	0.918	1	I: [0.352,6.346], 15	N/A	N/A

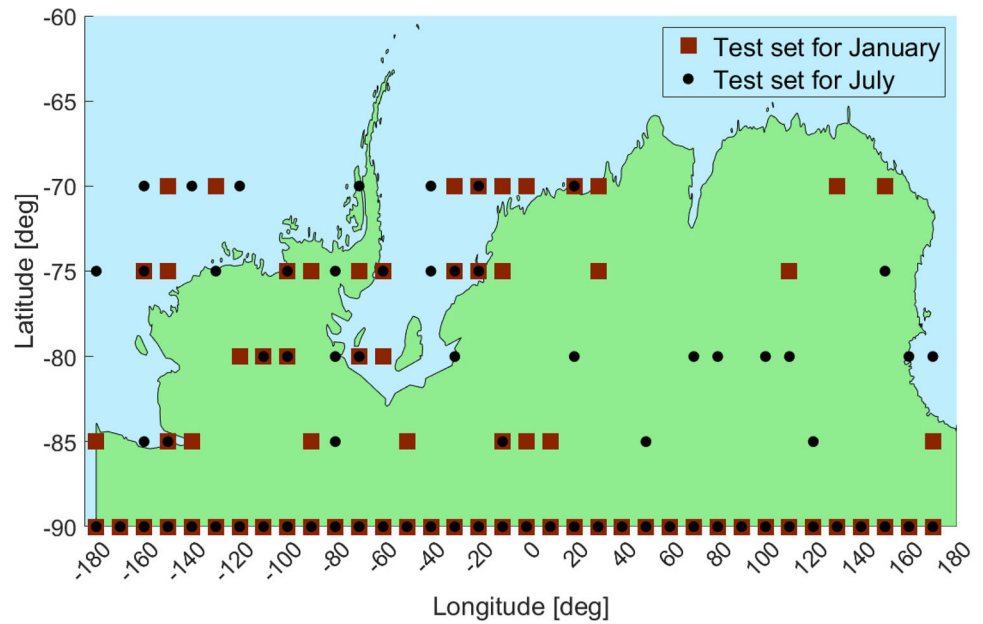
For each cloud (CL1/CL2/CL3), we report the cloud type (I for ICE and L for LIQUID), the cloud bottom and top heights in km, and the number of cloudy layers. Only samples with $\tau \leq 1$ are shown

Table 2 Cloud properties for the January dataset, reporting geolocation (LON/LAT), day number (DAY), total optical depth due to clouds (τ), and number of clouds (NC)

LON	LAT	DAY	τ	NC	CL1	CL2	CL3
−50	−85	17	0.030	1	I: [1.688, 3.238], 4	N/A	N/A
−10	−75	3	0.040	1	I: [2.596, 4.994], 4	N/A	N/A
10	−85	14	0.042	1	I: [2.631, 3.184], 2	N/A	N/A
110	−75	7	0.054	1	I: [3.207, 5.021], 3	N/A	N/A
N/A	−90	5	0.068	1	I: [2.788, 8.456], 8	N/A	N/A
20	−70	6	0.082	3	I: [0.432,1.312], 4	I: [2.033,4.937], 5	L: [0.862, 1.312], 2
130	−70	17	0.113	1	I: [2.570, 4.382], 4	N/A	N/A
−120	−80	6	0.149	1	I: [2.564, 7.453], 7	N/A	N/A
N/A	−90	17	0.164	2	I: [2.790, 3.867], 2	L: [2.790, 3.292], 1	N/A
−150	−75	6	0.197	2	I: [0.175, 1.993], 8	L: [0.819, 1.746], 4	N/A
−90	−85	5	0.262	1	I: [3.750, 7.528], 5	N/A	N/A
−90	−75	20	0.305	2	I: [1.369, 3.175], 5	L: [2.101, 3.175], 2	N/A
−110	−80	17	0.384	2	I: [1.812, 9.750], 12	L: [1.812, 2.163], 2	N/A
−160	−75	14	0.445	2	I: [0.075, 3.730], 12	L: [0.490, 1.145], 3	N/A
−70	−75	6	0.543	1	I: [1.820, 5.757], 7	N/A	N/A
−150	−70	11	0.612	2	I: [0.128, 1.906], 8	L: [0.544, 1.906], 6	N/A
−30	−75	9	0.688	2	I: [0.341, 2.660], 9	I: [3.798, 8.518], 6	N/A
30	−75	12	0.786	1	I: [1.312, 8.458], 7	N/A	N/A
N/A	−90	16	0.863	2	I: [2.789, 5.799], 5	L: [2.789, 3.223], 1	N/A
170	−85	2	0.898	1	I: [3.100, 8.362], 7	N/A	N/A

For each cloud (CL1/CL2/CL3) we report: the cloud type (I for ICE and L for LIQUID), the cloud bottom and top heights in km, and the number of cloudy layers. Only samples with $\tau \leq 1$ are shown

Fig. 7 Cloudy sky datasets for July (circles) and January (squares)



ditions. Specifically, the PWV influences the retrieval error in the FIR region, while surface temperature impacts the retrieval error in the atmospheric window.

7 Retrieval Error and Grid Step

In the FORUM spectral range, there are regions where there is no sensitivity to the emissivity under all atmospheric conditions. In these intervals, the random error approaches the a priori error. Also, the error profile for the finer grid contains intervals with significant oscillations. As pointed out

by Benyami et al. [27], there are micro-windows within the spectrum where the sensitivity is particularly pronounced. Conversely, there are wavelengths where the sensitivity is low due to their proximity to strong absorption lines of atmospheric gases.

The sensitivity tests shown in this paper use an emissivity retrieval grid with a step of 5 cm^{-1} . By using a coarser grid, the random error of the retrieval can be reduced, at the cost of a possibly increased smoothing error [16]. The increase is more noticeable when the actual surface emissivity shape presents sharp features.

To illustrate this point, we selected two cases, one in the Antarctic winter and one in the Sahara desert (case 1 in [13]),

Fig. 8 Surface emissivity average error, in the FIR spectral region, in July 2021 (a) and January 2021 (b), as a function of the total cloud optical depth. The color scale indicates the PWV

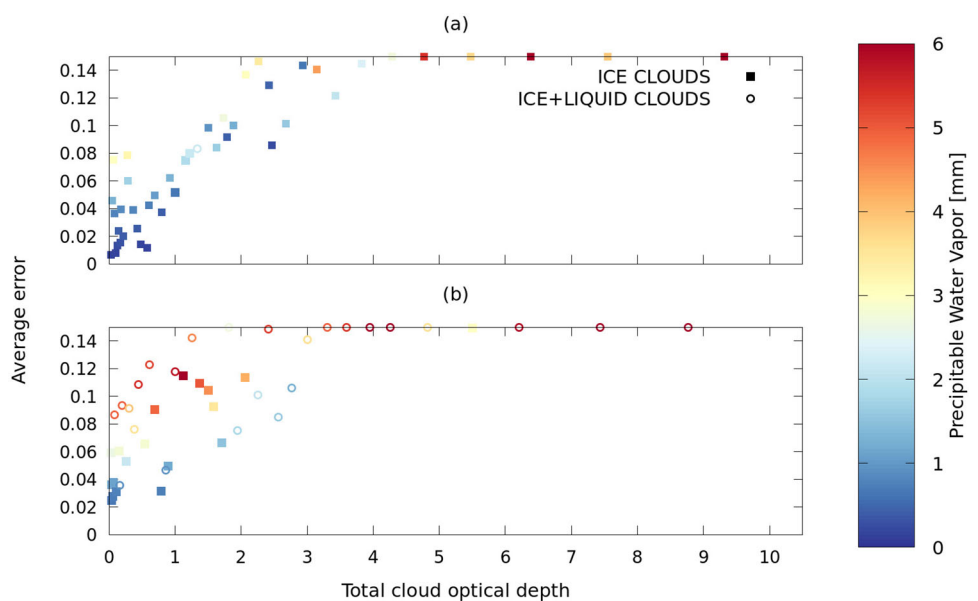
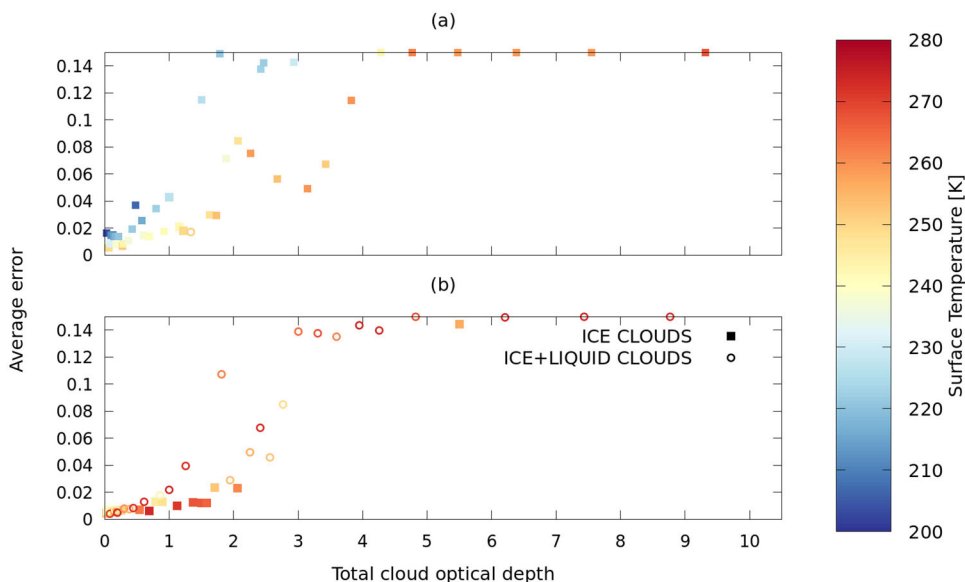


Fig. 9 Surface emissivity average error, in the atmospheric window, in July 2021 (a) and January 2021 (b), as a function of the total cloud optical depth. The color scale indicates the surface temperature



assuming true emissivities respectively given by the middle grains snow and desert Huang profiles [10]. We performed an actual retrieval using the same setting as in [13], and an a priori emissivity was obtained by subtracting 0.05 from the respective Huang true profile. For each of these scenarios, we performed two retrievals, one using an emissivity grid step of 5 cm^{-1} , and the other using an emissivity grid step of 25 cm^{-1} . The results of the retrievals are shown in Figs. 10 and 11. In each figure, panel (a) shows the true, the a priori, and the retrieved emissivity profiles with the respective error bars. In panel (b), we show the residuals of the fit, i.e., the differences between the synthetic observed spectrum and the spectrum simulated at the end of the retrieval iterations.

These differences are to be compared with the FORUM measurement noise level indicated by the black lines.

As expected, in the snow case where the emissivity profile has no sharp features, the coarser retrieval grid decreases the random error without introducing any significant smoothing error. The actual smoothing error is so small that the final value of the normalized χ^2 of this retrieval turns out to be even smaller than the value obtained with the finer emissivity retrieval grid.

On the other hand for the desert case, the coarser retrieval grid implies a significant smoothing error, i.e., the retrieval fails to reconstruct the sharp features of the true emissivity profile. The smoothing error due to the coarser retrieval grid

Fig. 10 Comparison between retrieval errors using different retrieval grids for a selected polar scenario on July 3rd, 2021, 12:00 UTC at longitude 80° and latitude -85° . A priori error and FORUM requirement are also shown

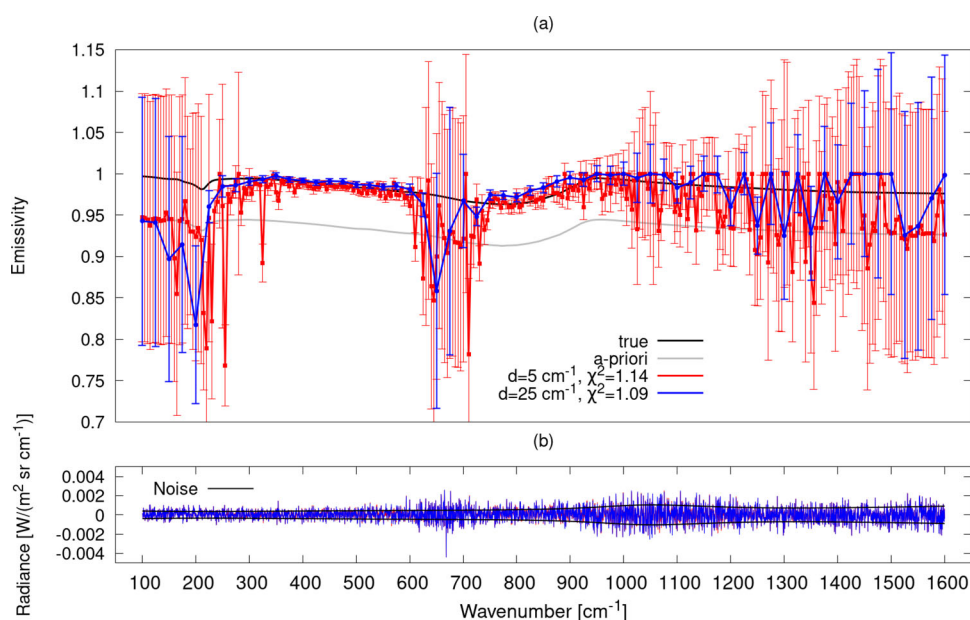
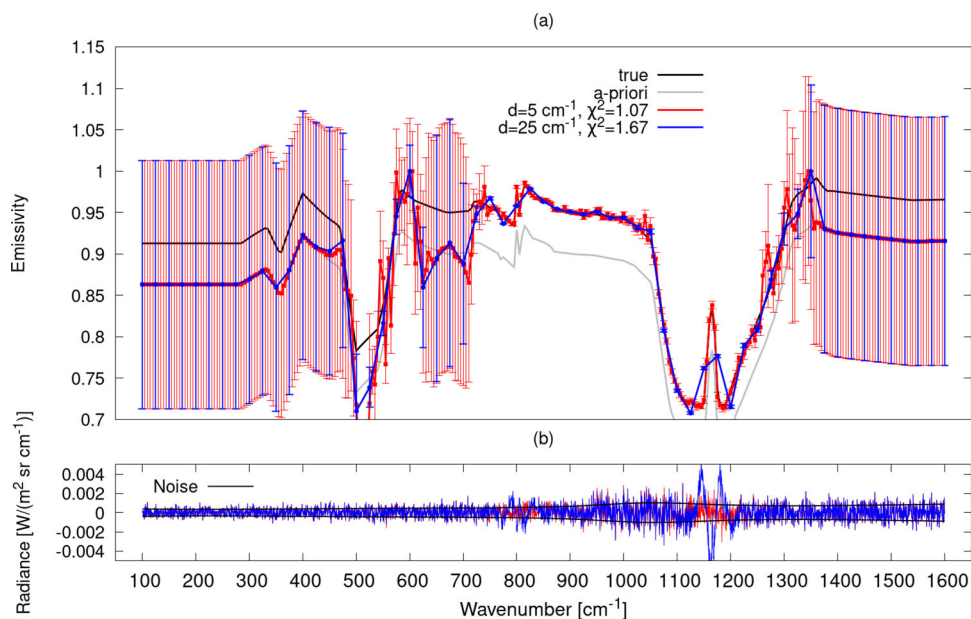


Fig. 11 Comparison between retrieval errors using different retrieval grids for a selected desert scenario on July 15th, 2017, 12:00 UTC at longitude 24.75° and latitude 24.75°. A priori error and FORUM requirement are also shown



in this case also produces residuals of the fit larger than the measurement noise error (see the bottom panel of Fig. 11).

8 Conclusions

In this paper we study the sensitivity of the FORUM simulated measurements to surface spectral emissivity. FORUM measurements are simulated using the current instrument specifications. The atmospheric and surface properties are extracted from the ERA5 reanalysis database.

In the FIR interval 300–600 cm^{-1} , the retrieval error is primarily influenced by the PWV in clear-sky conditions. This is due to the fact that this spectral region is dominated by the water vapor pure rotational band. Thus, this region becomes opaque for humidity-rich atmospheres. In dry atmospheres such as over the Antarctic plateau, FIR emissivity can be retrieved with an error less than 0.01 in clear-sky conditions. In cloudy conditions, reasonably small errors can be achieved over Antarctica for optically thin clouds, especially for small PWV values.

On the other hand, the atmospheric window at 800–950 cm^{-1} is not affected by strong gas absorption lines, thus it is transparent also for relatively humid atmospheres. In this case, a large thermal contrast between the surface and the lowest atmospheric layers improves the sensitivity of the measurements to the surface emissivity in clear sky conditions. In cloudy conditions, reasonably small errors can be achieved for optically thin clouds, particularly for high surface temperatures.

The retrieval errors presented in the paper are related to an emissivity retrieval grid with a step size of 5 cm^{-1} . Smaller random errors can be achieved by using a coarser retrieval grid, at the expense of a possibly increased smoothing error if

the actual emissivity shape contains sharp features, as illustrated by the test retrievals presented in Section 7. We believe that this trade-off between random and smoothing errors should be one of the factors driving the optimization of the retrieval grids for the operational processing.

Author Contribution M.R. and L.S. defined the problem to be studied and the methods to be employed. C.S., C.Z., and L.S. wrote the software used in the paper. C.S. and C.Z. extracted the atmospheric and surface scenarios analyzed from the ERA5 dataset. M.R. provided the hardware facilities to run the tests. C.S. ran all the tests and collected the results. All the authors contributed to writing and revising the paper.

Funding Open access funding provided by Consiglio Nazionale Delle Ricerche (CNR) within the CRUI-CARE Agreement. The work presented was supported by the CNR project: DIT.AD012.168, Support to the FORUM mission.

Data Availability The atmospheric and surface scenarios and numerical results of the tests presented in this paper are available at <https://doi.org/10.5281/zenodo.8410673>.

Declarations

Conflict of Interest The authors declare no competing interests.

Open Access This article is licensed under a Creative Commons Attribution 4.0 International License, which permits use, sharing, adaptation, distribution and reproduction in any medium or format, as long as you give appropriate credit to the original author(s) and the source, provide a link to the Creative Commons licence, and indicate if changes were made. The images or other third party material in this article are included in the article's Creative Commons licence, unless indicated otherwise in a credit line to the material. If material is not included in the article's Creative Commons licence and your intended use is not permitted by statutory regulation or exceeds the permitted use, you will need to obtain permission directly from the copyright holder. To view a copy of this licence, visit <http://creativecommons.org/licenses/by/4.0/>.

References

- Brindley HE, Harries JE (1998) The impact of far IR absorption on clear sky greenhouse forcing: sensitivity studies at high spectral resolution. *J Quant Spectrosc Radiative Transf* 60(2):151–180. [https://doi.org/10.1016/S0022-4073\(97\)00152-0](https://doi.org/10.1016/S0022-4073(97)00152-0)
- Kiehl JT, Trenberth KE (1997) Earth's annual global mean energy budget. *Bull Am Meteorol Soc* 78(2):197–208. [https://doi.org/10.1175/1520-0477\(1997\)078<0197:EAGMEB>2.0.CO;2](https://doi.org/10.1175/1520-0477(1997)078<0197:EAGMEB>2.0.CO;2)
- Collins WD, Mlynczak MG (2001) Prospects for measurement of far infrared tropospheric spectra: implications for climate modeling. In: AGU Fall Meeting Abstracts, vol 2001. pp GC32A–0210. <https://ui.adsabs.harvard.edu/abs/2001AGUFMGC32A0210C>. Accessed 26 Jan 2024
- Cox CV, Harries JE, Taylor JP, Green PD, Baran AJ, Pickering JC, Last AE, Murray JE (2010) Measurement and simulation of mid- and far-infrared spectra in the presence of cirrus. *Q J Roy Meteor Soc* 136:718–739. <https://doi.org/10.1002/qj.596>
- Lubin D, Chen B, Bromwich DH, Somerville RCJ, Lee W-H, Hines KM (1998) The impact of Antarctic cloud radiative properties on a GCM climate simulation. *J Climate* 11:447–462. [https://doi.org/10.1175/1520-0442\(1998\)011<0447:TIOACR>2.0.CO;2](https://doi.org/10.1175/1520-0442(1998)011<0447:TIOACR>2.0.CO;2)
- Baran AJ (2007) The impact of cirrus microphysical and macrophysical properties on upwelling far infrared spectra. *Q J Roy Meteor Soc* 133:1425–1437. <https://doi.org/10.1002/qj.132>
- Baran AJ (2009) A review of the light scattering properties of cirrus. *J Quant Spectrosc Radiat Transfer* 110:1239–1260. <https://doi.org/10.1016/j.jqsrt.2009.02.026>
- Palchetti L, Bianchini G, Natale GD, Guasta MD (2015) Far-infrared radiative properties of water vapor and clouds in Antarctica. *B Am Meteorol Soc* 96:1505–1518. <https://doi.org/10.1175/BAMS-D-13-00286.1>
- Huang Y, Ramaswamy V (2009) Evolution and trend of the outgoing longwave radiation spectrum. *J Clim* 22(17):4637–4651. <https://doi.org/10.1175/2009JCLI2874.1>
- Huang X, Chen X, Zhou DK, Liu X (2016) An observationally based global band-by-band surface emissivity dataset for climate and weather simulations. *J Atmos Sci* 73(9):3541–3555. <https://doi.org/10.1175/JAS-D-15-0355.1>
- Huang X, Chen X, Flanner M, Yang P, Feldman D, Kuo C (2018) Improved representation of surface spectral emissivity in a global climate model and its impact on simulated climate. *J Clim* 31(9):3711–3727. <https://doi.org/10.1175/JCLI-D-17-0125.1>
- Oetjen H (2019) Report for mission selection: FORUM. Tech. Rep. ESA-EOPSM-FORM-RP-3549, European Space Agency, ESA, 2200 AG, Noordwijk, The Netherlands. <https://esamultimedia.esa.int/docs/EarthObservation/EE9-FORUM-RfMS-ESA-v1.0-FINAL.pdf>. Accessed 26 Jan 2024
- Sgheri L, Belotti C, Ben-Yami M, Bianchini G, Carnicero Dominguez B, Cortesi U, Cossich W, Del Bianco S, Di Natale G, Guardabrazo T, Lajas D, Maestri T, Magurno D, Oetjen H, Raspollini P, Sgattoni C (2022) The FORUM end-to-end simulator project: architecture and results. *Atmos Meas Tech* 15(3):573–604. <https://doi.org/10.5194/amt-15-573-2022>
- Ridolfi M, Del Bianco S, Di Roma A, Castelli E, Belotti C, Dandini P, Di Natale G, Dinelli BM, C-Labonnote L, Palchetti L (2020) Forum Earth Explorer 9: characteristics of level 2 products and synergies with IASI-NG. *Remote Sens* 12(9). <https://doi.org/10.3390/rs12091496>
- Ridolfi M, Tirelli C, Ceccherini S, Belotti C, Cortesi U, Palchetti L (2022) Synergistic retrieval and complete data fusion methods applied to simulated FORUM and IASI-NG measurements. *Atmos Meas Tech* 15(22):6723–6737. <https://doi.org/10.5194/amt-15-6723-2022>
- Rodgers CD (2000) Inverse methods for atmospheric sounding. World Scientific, Oxford. <https://doi.org/10.1142/3171>
- Clough S, Shephard M, Mlawer E, Delamere J, Iacono M, Cady-Pereira K, Boukabara S, Brown P (2005) Atmospheric radiative transfer modeling: a summary of the AER codes. *J Quant Spectrosc Radiative Transf* 91(2):233–244. <https://doi.org/10.1016/j.jqsrt.2004.05.058>
- Sgheri L, Castelli E (2018) Speeding up the DISORT solver: mathematical approach and application to radiance simulations of FORUM. In: ESA ATMOS Conference, Salzburg. <https://doi.org/10.5281/zenodo.8119188>
- Stamnes K, Tsay SC, Wiscombe W, Jayaweera K (1988) Numerically stable algorithm for discrete-ordinate-method radiative transfer in multiple scattering and emitting layered media. *Appl Opt* 27:2502–2509. <https://doi.org/10.1364/AO.27.002502>
- Palchetti L, Bantges R, Buehler SA, Camy-Peyret C, Carli B, Cortesi U, Del Bianco S, Di Natale G, Dinelli BM, Feldman D, Huang XL, C-Labonnote L, Libois Q, Maestri T, Mlynczak MG, Murray JE, Oetjen H, Ridolfi M, Riese M, Russell J, Saunders R, Serio C, (2020) FORUM: unique far-infrared satellite observations to better understand how Earth radiates energy to space. *Bull Am Meteorol Soc* 1–52. <https://doi.org/10.1175/BAMS-D-19-0322.1>
- Hersbach H, Bell B, Berrisford P, Hirahara S, Horányi A, Muñoz-Sabater J, Nicolas J, Peubey C, Radu R, Schepers D, Simmons A, Soci C, Abdalla S, Abellan X, Balsamo G, Bechtold P, Biavati G, Bidlot J, Bonavita M, De Chiara G, Dahlgren P, Dee D, Diamantakis M, Dragani R, Flemming J, Forbes R, Fuentes M, Geer A, Haimberger L, Healy S, Hogan RJ, Hólm E, Janisková M, Keeley S, Laloyaux P, Lopez P, Lupu C, Radnoti G, de Rosnay P, Rozum I, Vamborg F, Villaume S, Thépaut JN, (2020) The ERA5 global reanalysis. *Q J R Meteorol Soc* 146(730):1999–2049. <https://doi.org/10.1002/qj.3803>
- Remedios JJ, Leigh RJ, Waterfall AM, Moore DP, Sembhi H, Parkes I, Greenough J, Chipperfield MP, Hauglustaine D (2007) MIPAS reference atmospheres and comparisons to v4.61/v4.62 MIPAS level 2 geophysical data sets. *Atmos Chem Phys Discuss* 7:9973–10017. <https://doi.org/10.5194/acpd-7-9973-2007>
- Wyser K (1998) The effective radius in ice clouds. *J Clim* 11(7):1793–1802. [https://doi.org/10.1175/1520-0442\(1998\)011<1793:TERIIC>2.0.CO;2](https://doi.org/10.1175/1520-0442(1998)011<1793:TERIIC>2.0.CO;2)
- Martin G, Johnson D, Spice A (1994) The measurement and parametrization of effective radius of droplets in warm stratocumulus clouds. *J Atmos Sci* 51:1823–1842. [https://doi.org/10.1175/1520-0469\(1994\)051<1823:TMAPOE>2.0.CO;2](https://doi.org/10.1175/1520-0469(1994)051<1823:TMAPOE>2.0.CO;2)
- Yang P, Gao BC, Baum BA, Wiscombe WJ, Hu YX, Nasiri SL, Soulen PF, Heymsfield AJ, McFarquhar GM, Miloshevich LM (2001) Sensitivity of cirrus bidirectional reflectance to vertical inhomogeneity of ice crystal habits and size distributions for two moderate-resolution imaging spectroradiometer (MODIS) bands. *J Geophys Res Atmos* 106(D15):17267–17291. <https://doi.org/10.1029/2000JD900618>
- Harries J, Carli B, Rizzi R, Serio C, Mlynczak M, Palchetti L, Maestri T, Brindley H, Masiello G (2008) The far-infrared Earth. *Rev Geophys* 46(4). <https://doi.org/10.1029/2007RG000233>
- Ben-Yami M, Oetjen H, Brindley H, Cossich W, Lajas D, Maestri T, Magurno D, Raspollini P, Sgheri L, Warwick L (2022) Emissivity retrievals with forum's end-to-end simulator: challenges and recommendations. *Atmos Meas Tech* 15(6):1755–1777. <https://doi.org/10.5194/amt-15-1755-2022>